Oral Diseases (2005) 11, 236–242

http://www.blackwellmunksgaard.com

ORIGINAL ARTICLE

Relationship between intracellular ROS production and membrane mobility in curcumin- and tetrahydrocurcumin-treated human gingival fibroblasts and human submandibular gland carcinoma cells

T Atsumi[1], S Fujisawa[2], K Tonosaki[1]

Departments of [1]Oral Physiology and [2]Oral Diagnosis, Meikai University School of Dentistry, Keyakidai, Sakado-shi, Saitama, Japan

OBJECTIVE: Curcumin is a well-known chemopreventive agent of oral cancers as well as stomach and intestinal cancers. The relationship between reactive oxygen species (ROS) production and cell membrane mobility was investigated to clarify the pro-oxidant mechanism of curcumin and tetrahydrocurcumin (TH-curcumin).

METHODS: The intracellular ROS production and membrane mobility by curcumin or TH-curcumin were measured in human submandibular adenocarcinoma cells (HSGs) and human primary gingival fibroblasts (HGFs). ROS and mobility were measured by 5-(and -6)-carboxy-2′,7′-dichlorofluorescein diacetate staining and fluorescence recovery after photo bleaching, respectively.

RESULTS: Curcumin produced ROS dose-dependently. ROS appeared in the region surrounding the cell membrane. The membrane mobility coefficient of the curcumin-treated cells was significantly lower than that of control cells. The lowered membrane mobility induced by curcumin was reversed by the addition of glutathione, an antioxidant. In contrast, TH-curcumin did not affect the ROS production or the membrane mobility coefficient. The alternations induced by curcumin treated HSG cells were greater than those by HGF cells.

CONCLUSION: The reduction in membrane mobility induced by curcumin was attributed to ROS production. The oxidative effects of curcumin may be related to the structure of the α, β-unsaturated carbonyl moiety as well as the phenolic OH group of this compound.

Oral Diseases (2005) **11**, 236–242

Keywords: curcumin; tetrahydrocurcumin; reactive oxygen species; membrane mobility; fluorescence recovery after photo bleaching

Correspondence: Dr T Atsumi, Department of Oral Physiology, Meikai University School of Dentistry, 1-1, Keyakidai, Sakado-shi, Saitama 350-0283, Japan. Tel: +81 49-279-2771; Fax: +81 49-287-4712; E-mail: tosi@dent.meikai.ac.jp
Received 15 April 2004; revised 30 June 2004; accepted 31 August 2004

Abbreviations: CDFH-DA, 5-(and -6)-carboxy-2′,7′-dichlorofluorescein diacetate; FRAP, fluorescence recovery after photo bleaching; HGF, human gingival fibroblast; HSG, human submandibular adenocarcinoma cell; NBD-PC, 1-acyl-2-(N-4-nitrobenzo -2-oxa-1,3-diazole) aminocaproyl phosphatidyl-choline; ROS, reactive oxygen species; TH-curcumin, tetrahydrocurcumin.

Introduction

Curcumin, 1, 7-bis (4-hydroxy-3-methoxyphenol)-1,6-heptadiene-3,5-dione (Figure 1), obtained from the rhizome of the plant *Curcuma longa*, is a naturally occurring pigment and component of the spice turmeric. Curcumin is of interest because of its anti-inflammatory and anti-carcinogenic activity (Satoskar *et al*, 1986; Donatus *et al*, 1990; Huang, 1997) and its action as a chemopreventive agent (Li and Lin-Shia, 2001; Ireson *et al*, 2002; Aggarwal *et al*, 2003).

Curcumin is a type of *ortho*-methoxyphenol, like eugenol (4-allyl-2 methyoxyphenol) used in the dental field. We previously reported the radical-producing and radical-scavenging activities, as well as the cytotocity, of *o*-methoxyphenols, demonstrating that these compounds act not only as antioxidants but also as prooxidants (Fujisawa *et al*, 2002). Also, we found that eugenol produced reactive oxygen species (ROS) under oxidative conditions with visible light irradiation or alkalization and enhanced its cytotoxicity through oxidation (Atsumi *et al*, 2001a). Curcumin-derived ROS production under oxidative conditions has been previously reported (Joe and Lokesh, 1994; Ahsan and Hadi, 1998; Nakamura *et al*, 1998; Ahsan *et al*, 1999; Bhaumik *et al*, 1999), however, the full quality, the mechanism of ROS production, and particularly, the distribution of intracellular ROS have not been precisely investigated.

In the present study, intracellular ROS was estimated by two different assays, i.e. flow cytometry using flouting cells to obtain quantitative data and adherent cell analysis and sorting system (ACAS) laser cytometry

Curcumin

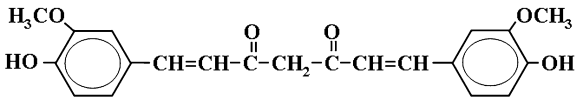

Tetrahydrocurcumin (TH-curcumin)

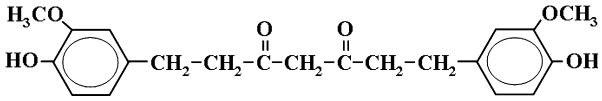

Figure 1 Chemical structure of curcumin and tetrahydrocurcumin

using adherent cells to obtain directly intact cell changes and to avoid trypsinization.

As curcumin is easily incorporated into cell membranes because of its high lipid solubility, curcumin might alter cell surface morphology, mobility, and adhesion. Such cellular reactions by curcumin may have inhibitory effects against oral carcinogenesis at the postinitiation stage. Curcumin has previously been reported to interact with egg and soy phosphatidylcholine that are models for the lipid bilayer of biological membranes (Began *et al*, 1999). Curcumin also modulates Fe-NTA (Ferric nitrilotriacetate) and hydrogen peroxide-induced peroxidation of microsomal membrane lipids and DNA damage (Iqbal *et al*, 2003). However, the direct interaction between curcumin and the cell membrane has not been studied. The technique of fluorescence recovery after photo bleaching (FRAP) is known as a suitable method to directly measure the diffusion behavior of cell membranes (Axelrod *et al*, 1976). Thus, we investigated the change in cell membrane mobility by curcumin using FRAP analysis.

As the cytotoxicity of curcumin focuses on cancerous cells, but not on normal cells, we used normal human primary gingival fibroblasts (HGFs) as well as cancerous human submandibular adenocarcinoma cells (HSGs) in this study. The anticancer activity of curcumin has been investigated using oral-squamous cell carcinoma, but the present study used HSGs cells because they tended to form a uniform monolayer and would thus probably give more reproducible effects on FRAP analysis.

Recently, tetrahydrocurcumin (TH-curcumin, Figure 1), a reduced derivative of curcumin and one of the major metabolites of curcumin, has been focused on for its cancer preventative activity (Leyon and Kuttan, 2003). TH-curcumin is converted from curcumin easily during digestion *in vivo* (Ravindranath and Chandrasekhara, 1981). TH-curcumin exhibits physiological and pharmacological properties of protective effects on oxidative stress as similar to those of curcumin *in vivo* (Sugiyama *et al*, 1996; Nakamura *et al*, 1998; Khopde *et al*, 2000; Naito *et al*, 2002).

To clarify the relationship between ROS production and membrane-fluidity behavior by curcumin based on a structure–activity relationship, in the present study we measured the intracellular ROS production, its cellular distribution and cellular membrane diffusion dynamics, i.e. the alteration of the mobility coefficient and recovery on curcumin or TH-curcumin treated HSGs or HGFs cells by using the FRAP technique.

Materials and methods

Chemicals

The following chemicals and reagents were obtained from the indicated companies: curcumin [1,7-bis(4-hydroxy-3-methoxyphenol)-1,6-heptadiene-3,5-dione], from Tokyo Kasei Chem. Co., Tokyo, Japan; 5-(and -6)-carboxy -2′,7′-dichlorofluorescein diacetate (CDFH-DA) and 1-acyl-2-(N-4-nitrobenzo-2-oxa-1,3-diazole) aminocaproyl phosphatidyl-choline (NBD-PC), from Molecular Probes Inc., Eugene, OR, USA; and MTT [3-(4, 5–dimethyl-2-thiazolyl)-2, 5-diphenyltetrazolium bromide] kit, from Promega Co., Madison, WI, USA. TH-curcumin was kindly donated by Dr I. Yokoe of Josai University. The chemical structures of curcumin and TH-curcumin are shown in Figure 1.

Cells and cell culture

We previously intensively investigated to clarify the cytotoxic effects of methoxyphenols such as curcumin has been previously reported to be enhanced by their intermediates, i.e. quinonemethides and quinones formed via oxidation (Fujisawa *et al*, 2002, 2004) on HSG and HGF cells. So, we used HSG and HGF cells in the present study.

Human primary gingival fibroblasts were cultured by the method of Kawase *et al* (1994) from a fragment of the gingiva attached to a supernumerary tooth extracted from a 7-year-old female patient. Informed consent from the patient and her parents was obtained, as was ethical clearance for the study from the Ethics Committee of the Meikai University School of Dentistry. The tissue was cut into 1–2 mm^3 pieces, which were then washed twice with phosphate-buffered saline supplemented with 100 U ml^{-1} penicillin and 100 μg ml^{-1} streptomycin and placed into tissue culture dishes. The explants were incubated for about 3 weeks at 37°C in culture medium consisting of Minimum Essential Medium α modification (α-MEM) containing 30% fetal bovine serum (FBS) in a humidified atmosphere of 5% carbon dioxide in air. The outgrowths were then subcultured by trypsinization and passaged in α-MEM supplemented with 10% FBS. The HGF cells, having a uniform structure of fibroblasts, were used in passage numbers 5–7.

The HSG cell line (Shirasuna *et al*, 1981) was donated by Dr M. Satoh of Tokushima University. HSG cells were cultured in MEM supplemented with 10% FBS.

Detection of intracellular ROS production

ROS was measured by dichlorofluorescein assay (Boissy *et al*, 1989) in both adherent cell and flow cytometetic analysis. Briefly, CDFH-DA is a non-fluorescent and stable ester compound that readily diffuses through cell membrane. Intracellularly, cytosolic esterase enzymes cleave the acetate moiety, and the resultant hydrolyzed

compound is trapped within the cell. In the presence of peroxides or hydroperoxide, the compound is oxidized to the highly fluorescent form of 5-(and -6)-carboxy-2′,7′-dichlorofluorescein (CDF). As all ROS form peroxide in living cells, these species were detected by measurement of the fluorescence intensity of CDF.

Flow cytometry on flouting cell

This was modified from our previous report (Atsumi *et al*., 2001b).

In the case of quantitative analysis, HGF or HSG cells were seeded at 1×10^5 cells per 2 ml of MEM with 10% FBS in each well of a 6-well plate and cultured for 2 days to reach semi confluence. The cells were then washed twice with Hanks buffered saline solution (HBSS, pH 7.4) and kept in the solution for 60 min before the assay. If the medium was not replaced with HBSS, the level of ROS produced was higher, but the results were not reproducible. Curcumin or TH-curcumin was added 1–30 μM to the cells, which were then incubated for 30 min. Next, 10 μM CDFH-DA was added to each well, after which the cells were incubated at 37°C for 30 min. The cells were then detached by use of trypsin solution and washed with HBSS. Next, they ($2–4 \times 10^5$) were suspended in 0.5 ml of HBSS, and the intensity of CDF at 520–530 nm (PMT 2) of 5000 individual cells was measured with a flow cytometer (Beckman ALTRA, Miami, FL, USA). ROS values were obtained from the X-mean of PMT 2 of the flow cytometric distribution chart. To minimize the effect of auto fluorescence of HSG cells and HSG cells, we adjusted the PMT 2 of each control sample to 1.0 by changing its voltage. Some scavengers of ROS, such as N-acetyl-L-cysteine (NAC), glutathione (GSH), mannitol, sodium azide, catalase (from bovine), and superoxide dismutase (SOD) (from bovine erythrocytes) were added separately to the cells 1 h before the addition of curcumin.

ACAS laser cytometry on adherent cells

The ACAS laser cytometry was performed to obtain directly intact cell changes and to avoid trypsinization using adherent cell. HSG or HGF cells were inoculated into 35-mm glass-bottom dishes at a density of 3×10^4 cells in 1 ml of MEM supplemented with 10% FBS, and were cultured at 37°C for 2 days. The cells were then washed twice with serum-free medium. Both 10 μM CDFH-DA and 5 or 10 μM curcumin or 10 μM TH-curcumin were added to the dish, and the cells were then incubated for 30 min. The cells were washed and then analyzed with an ACAS 570 laser cytometer (Meridian Inc, Okemos, MI, USA), a computer-controlled scanning laser instrument operated by an image analysis program. The instrument was equipped with an argon laser set at 488 nm, and the emission at 530 ± 30 nm (CDF intensity) was recorded as a pseudo-color from two-dimensional image scans.

Fluorescence recovery after photo bleaching analysis

The FRAP is made with a short intense pulse of light from an argon ion laser, and recovery of fluorescence within the bleached area is subsequently measured by repetitive scanning across the cell surface with an attenuated laser beam of an ACAS laser cytometer. HSG or HGF cells were inoculated into 35-mm glass-bottom dishes at a density of 1×10^4 cells in 1 ml of MEM supplemented with 10% FBS, and cultured at 37°C overnight. The cells were washed with serum free MEM twice 1 h before the experiment. Curcumin or TH-curcumin at 10 μM was then added to the cells, and the cells were incubated for 30 min and thereafter labeled with NBD-PC, a fluorescent indicator of a naturally occurring membrane lipid, phosphatidylcholine, used at 10 μM (4°C for 15 min on ice) for the purpose of staining only the cell membrane. The cells were washed with HBSS and immediately transferred to the ACAS work station. In the FRAP program, a pseudo color two-dimensional image can be obtained to visualize the distribution of the fluorophore, and to determine the start, end, and bleach positions, as indicated by 'a,' 'b,' and 'c,' respectively, in Figure 2a. The computer-controlled stage automatically positions itself according to these coordinates. Prebleach line scan (Figure 2b) were made in order establish the initial fluorescence intensity profile. Recovery of fluorescence occurred if unbleached fluorescent molecules from the surrounding regions were free to diffuse into this area. A selected small area was irradiated with a larger high intensity beam, and the recovery of fluorescence was monitored with postbleach scans by line scans (Figure 2c). Analysis was performed with a modified round type of program. The recovery curve (μ value curve) was then drawn (Figure 2d) and finally, the coefficient of mobility, i.e. the diffusion constant and/or flow velocity, and the rate recovery of fluorescence were obtained using the computer program included with the FRAP program.

Data analysis

Statistical comparisons of the effects of curcumin and TH-curcumin on ROS levels and membrane mobility were made using a Student's *t*-test.

Results

Curcumin- and TH-curcumin-elicited ROS production and distribution of ROS in HGFs and HSGs

Figure 3 shows the ROS production induced in HGF and HSG cells by treatment with 1–30 μM curcumin or TH-curcumin for 1 h obtained from inserted flow cytometric data. Curcumin induced ROS production dose dependently from 1 to 30 μM in both HSG and HGF cells. In detail, ROS production of curcumin was greater in HSG cells than in HGF cells. In contrast, TH-curcumin did not produce any ROS in either cell type. To elucidate the events involved in curcumin-stimulated ROS production, we examined the inhibitory effects of various antioxidants on ROS production in HSG cells elicited by treatment with 30 μM curcumin for 1 h (Table 1). Catalase (H_2O_2 inhibitor), mannitol (a specific inhibitor of hydroxyl radical), sodium azide (a specific inhibitor of singlet

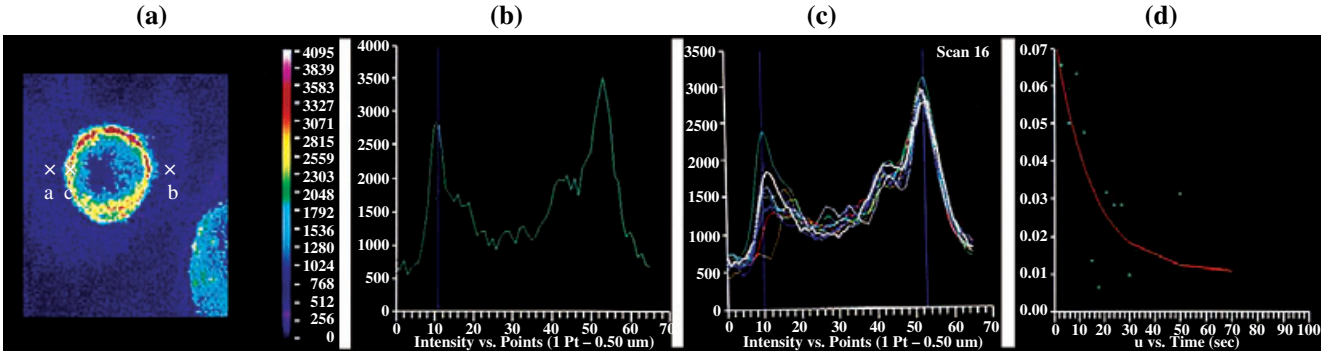

Figure 2 Fluorescence recovery after photo bleaching (FRAP) analysis method. An example of curcumin-treated human submandibular adenocarcinoma cells (HSGs) subjected to FRAP analysis using an adherent cell analysis and sorting system (ACAS) laser cytometer. HSG were inoculated into 35-mm glass-bottom dishes, cultured at 37°C overnight, then pretreated with curcumin (10 μM) for 30 min. Thereafter, they were labeled with NBD-PC (10 μM), at 4°C for 15 min. The cells were transfered to the ACAS workstation run by the FRAP program. (**a**) Pseudocolor representation of the two-dimensional image of a prebleach scan, and the '×' symbols show the start 'a', end 'b', and bleach 'c' positions. The small selected area (c) was irradiated with a high intensity larger beam, and the recovery of fluorescence was monitored with postbleach scans 10 times per 3 s and 6 times per 20 s. (**b**) Line scan at prebleach. The blue line indicates the bleached point at the 'c' position in (**a**). (**c**) All of the line scans recovered, that is, prebleach (green line), just after irradiation (orange line), after the first recovery (red line) and last recovery (white line). The left bleached edge point showed recovery, in contrast, that of the right edge, which was not bleached, remained steady. (**d**) Recovery curve (μ value curve) obtained from (**c**). Conditions for the detection: step size, 0.5 μm; x scan, 100; y scan, 100; PMT, 40%; scan strength, 5%; blast strength, 100%; blast time, 15 ms; laser power, 100 mW

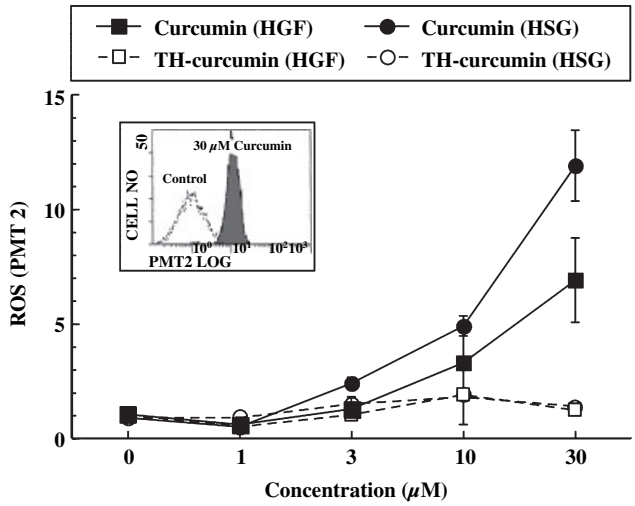

Figure 3 Reactive oxygen species (ROS) production of curcumin- or tetrahydrocurcumin (TH-curcumin)-treated human primary gingival fibroblast and human submandibular adenocarcinoma cells (HSG). Cells (1×10^5) were incubated in a medium containing 10% fetal bovine serum for 2 days, then washed with Hans buffered saline solution (HBSS). Curcumin or TH-curcumin (1–30 μM) was added to the cells, and incubation was carried out for 1 h. The cells were then stained with 10 μM 5-(and -6)-carboxy-2′,7′-dichlorofluorescein diacetate (CDFH-DA) for 30 min. Cells were harvested with trypsin solution and washed with HBSS. Amounts of intracellular ROS were estimated by using a flow cytometer (Beckmann, ALTRA), which measured the fluorescence intensity of CDF (520–530 nm, PMT 2 of the flow cytometer). The insert shows a typical flow cytometric fluorescence distribution (PMT 2), with the white area being the control sample and the colored area, 30 μM curcumin-treated HSG cells. ROS values were obtained from the mean of PMT 2 and expressed as control cells taken as 1. Data are the average ± SD of three or five different experiments

Table 1 Effects of various inhibitors on reactive oxygen species (ROS) production by curcumin-treated human submandibular adenocarcinoma cells (HSGs)

Treatment	*ROS (%)*
Curcumin (30 μM)	100.0 ± 14.60
Curcumin (30 μM) + SOD	98.3 ± 13.40
Curcumin (30 μM) + Catalase	37.5 ± 3.40***
Curcumin (30 μM) + Mannitol	80.4 ± 1.38*
Curcumin (30 μM) + NaN_3	46.1 ± 2.29***
Curcumin (30 μM) + NAC	52.5 ± 7.25***
Curcumin (30 μM) + GSH	44.1 ± 3.86***

Inhibitors were added to HSG cells 1 hour before the addition of 30 μM curcumin. ROS production was measured similarly to Figure 3. The value of ROS production was expressed as % of the 30 μM curcumin-treated HSG cell sample taken as 100. Concentrations of inhibitors were as follows: superoxide dismutase (SOD), 500 U; catalase, 500 U; mannitol, 10 mM; sodium azide (NaN_3), 50 mM; N-acetyl-l-cysteine (NAC), 5 mM; glutathione (GSH), 5 mM. Data are average ± SD of three or four different experiments. ***$P > 0.001$; *$P > 0.05$ *vs* curcumin-treated sample without inhibitor.

oxygen), and antioxidants (N-acetyl-L-cysteine and GSH) effectively reduced the level of curcumin-produced ROS, whereas SOD had no effect. Surely this may be because SOD catalyses the dismutation of superoxide to form H_2O_2 and therefore, SOD will have no effect on reducing H_2O_2 formation.

Next, to clarify the distribution of ROS in the cells, we measured intracellular ROS production using adherent cells. Figure 4 shows typical two-dimensional image-scan data as the pseudo-colors of CDF intensity for ROS produced in the adherent HSG and HGF cells treated with curcumin or TH-curcumin. Curcumin apparently produced ROS in the cytoplasm surrounding cell membranes. High ROS production was observed in the cells treated with curcumin, but not those treated with TH-curcumin. HSG cells produced much more ROS than the HGF ones. The average fluorescence of curcumin- and TH-curcumin-treated single cells determined by the computer

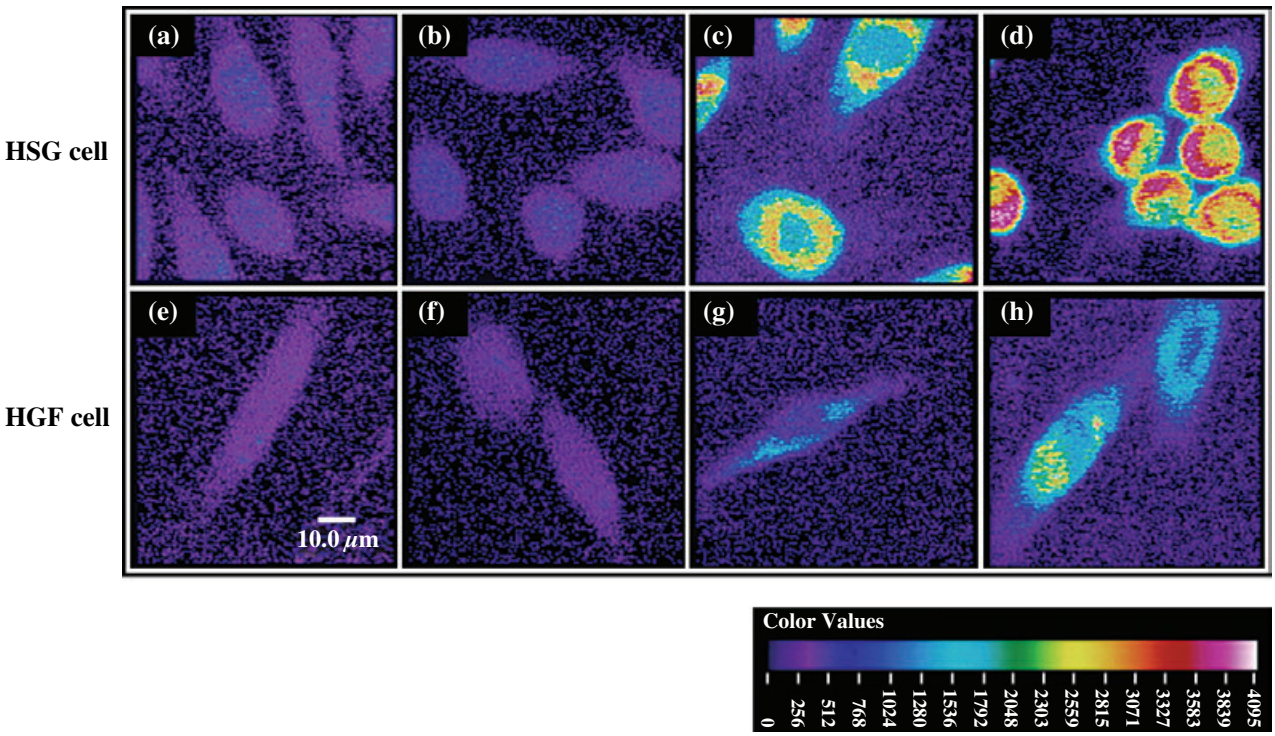

Figure 4 Typical 2-dimensional image scans (in pseudo color) of reactive oxygen species produced by curcumin or tetrahydrocurcumin (TH-curcumin) in human submandibular adenocarcinoma cells (HSGs) or human primary gingival fibroblast (HGF) cells obtained by adherent cell analysis and sorting system (ACAS) 570 laser cytometry. HSG and HGF cells (3×10^4 ml^{-1}) were cultured in MEM containing 10% fetal bovine serum for 2 days. Both 10 μM 5-(and -6)-carboxy-2′,7′-dichlorofluorescein diacetate and 5 or 10 μM curcumin or TH-curcumin were added to the cells, and cells were then incubated at 37°C for 30 min. An image scan of the cells was immediately obtained with a laser cytometer. Photos '**a**' and '**e**' are the control; '**b**' and '**f**,' are cells treated with 10 μM TH-curcumin; '**c**' and '**g**,' with 5 μM curcumin; and '**d**' and '**h**,' with 10 μM curcumin. Photos '**a**'–'**d**' are HSG cells; and '**e**'–'**h**,' HGF cells. Conditions for the detection of the ACAS 570: step size, 0.5 μm; x scan, 150; y scan, 150; PMT, 40%; scan strength, 50%; laser power, 100 mW

program was 405 (control, photo 'a' in Figure 4), 419 (10 μM TH-curcumin, 'b'), 1741 (5 μM curcumin, 'c'), and 2408 (10 μM curcumin, 'd') for HSG cells, and 216 (control, 'e'), 258 (10 μM TH-curcumin, 'f'), 637 (5 μM curcumin, 'g'), and 1154 (10 μM curcumin, 'h') for HGF cells. These values were paralleled by the flow cytometric ROS level shown in Figure 2.

Effects of curcumin and TH-curcumin on the lateral diffusion of the cell membrane

Table 2 shows the lateral diffusion of the fluorescent lipid probe in the cell membrane (mobility coefficient and rate of recovery of fluorescence) of HSG or HGF cells when the cells were treated with 10 μM curcumin or TH-curcumin for 30 min, as calculated from the FRAP data shown in Figure 2. The correlation coefficient for all experiments was within 0.02. The mobility coefficients (10^{-8} cm^2 s^{-1}) obtained with curcumin (1.73 ± 0.60 for HSG and 1.25 ± 0.51 for HGF) were significantly lower than those of the control (3.43 ± 1.49, HSG, $P < 0.001$; 1.98 ± 1.14, HGF, $P < 0.05$). The value for curcumin on the HSG cells was significantly reversed by the addition of GSH ($P < 0.05$), whereas the coefficients obtained with TH-curcumin (3.57 ± 1.46, HSG; 2.03 ± 0.90, HGF) were not significantly different from those of controls. The rate of recovery (%) for both curcumin and TH-curcumin was 70–75% and was not significantly different from controls.

Table 2 Mobility coefficient and rate of recovery of fluorescence in curcumin- and tetrahydrocurcumin (TH-curcumin)-treated human submandibular adenocarcinoma cell (HSG) or human primary gingival fibroblast (HGF) cells as determined by fluorescence recovery after photo bleaching (FRAP) analysis

	Mobility coefficient ($\times 10^{-8}$ *cm^2 s^{-1}*)	*Rate of recovery (%)*
HSG cell		
Control	3.43 ± 1.49	71.3 ± 9.2
Curcumin (10 μM)	1.73 ± 0.60***	75.3 ± 18.2
Curcumin (10 μM) + GSH (1 mM)	2.69 + 1.24†	74.4 ± 17.8
TH-curcumin (10 μM)	3.57 ± 1.46	69.2 ± 16.0
HGF cell		
Control	1.98 ± 1.14	72.5 ± 15.8
Curcumin (10 μM)	1.25 ± 0.51*	73.4 ± 16.2
TH-curcumin (10 μM)	2.03 ± 0.90	71.3 ± 17.7

HSG or HGF cells were incubated with curcumin (10 μM) or TH-curcumin (10 μM) for 30 min. FRAP analysis was carried out as described in Figure 2. Glutathione (GSH, 1 mM) was added before 1 hour addition of curcumin or TH-curcumin. Student *t*-test was performed 10 independent experiments except for minimum and maximum value. ***$P > 0.001$; *$P > 0.05$ *vs* the controls and †$P < 0.05$ *vs* the curcumin-treated HSG cells.

Discussion

Curcumin produced ROS efficiently on cell membranes in both HSG and HGF cells (Figures 3 and 4). The present findings are in agreement with those previously reported (Joe and Lokesh, 1994; Ahsan and Hadi, 1998; Ahsan *et al*, 1999; Bhaumik *et al*, 1999), despite differences in the cells and experimental conditions. To detect ROS production, we used a combination of CDFH-DA, which is a peroxide or hydrogen peroxide probe, and ACAS laser cytometry, which was capable of directly detecting the ROS distribution in the cell. Focusing on the ROS distribution on biological membranes allowed us to interpret the possible alteration in the membrane structure or morphology. Actually, the lateral diffusion of lipid in the membranes of the curcumin-treated HSG and HGF cells was reduced, compared with that of controls or TH-curcumin-treated cells (Table 2), as judged from the results obtained by using the FRAP technique. Also, the diffusion coefficient was reduced by curcumin and recovered by the addition of GSH, a powerful antioxidant (Table 2). A positive correlation was found between ROS production and the decrease in the diffusion coefficient, possibly because of the lipid peroxidation of unsaturated lipids in membranes induced by ROS. However, there is little information about the effect of curcumin on direct lipid peroxidation in cell membranes. Several researchers previously reported that curcumin reduced lipid peroxidation induced by H_2O_2 and so (Khopde *et al*, 2000; Venkatesan and Rao, 2000; Iqbal *et al*, 2003), suggesting that curcumin itself acted as an antioxidant. Conversely, in the present study curcumin promoted lipid peroxidation in cell membranes. Curcumin seemed to preferably act as a pro-oxidant, which was possibly related with the formation of ROS and consequently, the less GSH level. Chlorogenic acid (a curcumin-related compound)-induced lipid peroxidation was previously reported to be detected by measuring 4-hydroxynonenal, which is a decomposition product of lipid peroxidation derived from polyunsaturated fatty acids (Sakiyama and Yamasaki, 2002). Also, curcumin is well known to induce apoptotic death (Khar *et al*, 2001; Morin *et al*, 2001) and to exhibit phosphatidylcholine exposure induced by a flip flop in the lipid bilayer as an early apoptosis sign (Bhaumik *et al*, 1999). Together with these findings, curcumin-induced lipid peroxidation of biological membranes may be associated with ROS production of this compound.

In the present study, increasing ROS production and decreasing membrane mobility for curcumin-treated cells was observed not only in cancer cells (HSG) but also in normal cells (HGF). Such an alteration was much more prevalent in HSG cells than in HGF cells. Thus, it is clear that such changes were caused by nonspecific effects of curcumin on cellular membranes, in both normal and cancer cells.

On the contrary, TH-curcumin did not undergo ROS production or membrane fluidity (Figures 3 and 4 and Table 2). We recently found that the cytotoxicity of curcumin was about twofold greater than that of TH-curcumin, that is, the CC_{50} (μM) of curcumin and TH-curcumin against HSG cells were 85.3 and 113.4, respectively, whereas those of corresponding HGF cells were 62.3 and 164.2, respectively (data not shown). In addition, we also investigated that the cytotoxicity of visible-light irradiated curcumin was one order of magnitude greater than that of the TH-curcumin counterpart, whereas that of curcumin in the presence of horseradish peroxidase was significantly less than that of TH-curcumin (data not shown), possibly due to the binding of the horseradish peroxidase heme environment with chelatable curcumin. Horseradish peroxidase (donor H_2O_2 oxidoreductase) is a hemoprotein enzyme that primarily catalyzes the oxidation of a wide variety of donor molecules by hydrogen peroxidase. These findings suggest that the cytotoxic mechanism of TH-curcumin might be different from that of curcumin involving ROS production. TH-curcumin, without double bonds in the α, β carbonyl moiety, did not produce ROS and less membrane fluidity, in contrast, curcumin with the α, β carbonyl moiety produced much more ROS and alterations in membrane fluidity, suggesting that curcumin has a high oxygen affinity. We recently demonstrated that curcumin preferably scavenged peroxyradicals, but not alkylradicals, and underwent dimerization from curcumin monomers via radical oxidization, strongly suggesting that curcumin is a potent scavenger of peroxyradicals derived from unsaturated phosphatidyl lipids in biological membranes and that curcumin might have adverse effects on nucleophiles in proteins during the oxidation process (Fujisawa *et al*, 2004).

As a prooxidant, TH-curcumin is different from curcumin, however, as an antioxidant, TH-curcumin is known to be similar to curcumin (Khopde *et al*, 2000; Li and Lin-Shia, 2001; Ireson *et al*, 2002). TH-curcumin may be useful as a chemopreventitive agent of cancers and anti-inflammatory agents.

References

Aggarwal BB, Kumar A, Bharti AC (2003). Anticancer potent of curcumin: preclinical studies. *Anticancer Res* **29:** 363–398.

Ahsan H, Hadi SM (1998). Strand scission in DNA induced by curcumin in the presence of Cu(II). *Cancer Lett* **124:** 23–30.

Ahsan H, Parveen N, Khan NU *et al* (1999). Pro-oxidant, anti-oxidant and cleavage activities on DNA of curcumin and its derivatives demethoxycurcumin and bis-demethoxycurcumin. *Chem-Bioll Int* **121:** 161–175.

Atsumi T, Iwakura I, Fujisawa S *et al* (2001a). Reactive oxygen species generation and photo-cytotoxicity of eugenol in solutions of various pH. *Biomaterials* **22:** 1459–1466.

Atsumi T, Iwakura I, Fujisawa S *et al* (2001b). The production of reactive oxygen species by irradiated camphorquinone-related photosensitizers and their effect on cytotoxicity. *Arch Oral Biol* **46:** 391–401.

Axelrod D, Koppel DE, Schlessinger J *et al* (1976). Mobility measurement by analysis of fluorescence photo bleaching recovery kinetics. *Biophys J* **16:** 1055–1069.

Began G, Sudharshan E, Udaya SK *et al* (1999). Interaction of curcumin with phosphatidyl cholin: a spectrofluorometric study. *J Agric Food Chem* **47:** 4992–4997.

Bhaumik S, Anjum R, Rangaraj N *et al* (1999). Curcumin mediated apoptosis in AK-5 tumor cells involves the production of reactive oxygen intermediates. *FEBS Lett* **456:** 311–314.

Boissy RE, Trinkle LS, Nordlund JJ (1989). Separation of pigmented and albino melanocytes and the concomitant evaluation of endogenous peroxide content using flow cytometry. *Cytometry* **10:** 779–787.

Donatus IA, Sardjoko, Vermeulen NP (1990). Cytotoxic and cytoprotective activities of curcumin: Effects on paracetamol-induced cytotoxicity, lipid peroxidation and glutathione depletion in rat hepatocytes. *Biochem Pharmacol* **39:** 1869–1875.

Fujisawa S, Atsumi T, Kadoma Y (2002). Antioxidant and prooxidant action of eugenol-related compounds and their cytotoxicity. *Toxicology* **177:** 39–54.

Fujisawa S, Atsumi T, Ishihara M *et al* (2004). Cytotoxicity, ROS-generation activity and radical-scavenging activity of curcumin and related compounds. *Antcancer Res* **24:** 563–570.

Huang M-T (1997). Antioxidant and antitumorgenic properties of curcumin. In: Ohigashi H, Osawa T, Terao S, Watanabe S, Yoshikawa T, eds. *Food Factors for Cancer Prevention*. Springer: Tokyo, pp. 249–252.

Iqbal M, Okazaki Y, Okada S (2003). In vitro curcumin modulates ferric nitrilotriacetate (Fe-NTA) and hydrogen peroxide (H_2O_2)-induced peroxidation of microsomal membrane lipids and DNA damage. *Teratog Carcinog Mutagen* **23**(Suppl. 1)**:** 151–160.

Ireson CR, Jones DJ, Orr S *et al* (2002). Metabolism of the cancer chemopreventive agent curcumin in human and rat intestine. *Cancer Epidermiol Biomarkers Prev* **11:** 105–111.

Joe B, Lokesh BR (1994). Role of capsaicin, curcumin and dietary n-3 fatty acids in lowering the generation of reactive oxygen species in rat peritoneal macrophages. *Biochim Biophy Acta* **1224:** 255–263.

Kawase T, Sato S, Miake K *et al* (1994). Alkaline phosphatase of human periodontal ligament fibroblast-like cells. *Adv Dent Res* **2:** 234–239.

Khar A, Ali AM, Parhasaradhi BV *et al* (2001). Induction of stress response renders human tumor cell lines resistant to curcumin–mediated apoptosis; Role of reactive oxygen intermediates. *Cell Stress Chaperones* **6:** 368–376.

Khopde SM, Priyadarsini KI, Guha SN *et al* (2000). Inhibition of radiation-induced lipid peroxidation by tetrahydrocurcumin: possible mechanisms by pulse radiolysis. *Biosci Biotechno Biochem* **64:** 503–509.

Leyon PV, Kuttan G (2003). Studies on the role of some synthetic curcuminoid derivatives in the inhibition of tumour specific angiogenesis. *J Exp Clin Cancer Res* **22:** 77–83.

Li JK, Lin-Shia SY (2001). Mechanisms of cancer chemoprevention by curcumin. *Proc Natl Sci Counc Repub China* **B25:** 59–66.

Morin D, Barthelemy S, Zini R *et al* (2001). Curcumin induces the mitochondrial permeability transition pore mediated by membrane protein thiol oxidation. *FEBS Lett* **495:** 131–136.

Naito M, Wu X, Nomura H *et al* (2002). The protective effects of tetrahydrocurcumin on oxidative stress in cholesterol-fed rabbits. *J Atheroscler Thomb* **9:** 243–250.

Nakamura Y, Ohto Y, Murakami A *et al* (1998). Inhibitory effects of curcumin and tetrahydrocurcuminoids on the tumor promoter-induced reactive oxygen species generation in leukocytes in vitro and in vivo. *Jpn J Cancer Res* **89:** 361–370.

Ravindranath V, Chandrasekhara N (1981). In vitro studies on the intestinal absorption of curcumin in rats. *Toxicology* **20:** 251–257.

Sakiyama Y, Yamasaki H (2002). Lipid peroxidation induced by phenolics in conjugation with aluminum ions. *Biol Plant* **45:** 249–254.

Satoskar RR, Shah SJ, Shenoy SG (1986). Evaluation of anti-inflammatory property of curcumin (diferuloyl methane) in patients with postoperative inflammation. *Int J Clin Pharmacol Theor Toxic* **24:** 651–654.

Shirasuna K, Sato M, Miyazaki T (1981). A neoplastic epithelial duct cell line established from an irradiated human salivary gland. *Cancer* **48:** 745–752.

Sugiyama Y, Kawakishi S, Osawa T (1996). Involvement of the beta-diketone moiety in the antioxidative mechanism of tertrahydrocurcumin. *Biochem Pharmaco* **23:** 519–525.

Venkatesan P, Rao MN (2000). Structure-activity relationships for the inhibition of lipid peroxidation and scavenging of free radicals by synthetic symmetrical curcumin analogues. *J Pharm Pharmacol* **52:** 1123–1128.